V.2. Dilute Gases

Dynamical systems of many particles are difficult to treat in any detail. Substantial efforts are expended by the modern physical chemistry community to develop practical approaches to understand and predict strongly coupled, multi-dimensional quantal systems, for example, in the framework of molecular-dynamics and other transport models. A later section will discuss and illustrate basic foundations of such models. These models explain in heuristic fashion, how an asymptotic equilibrium state of such systems is reached and what its detailed properties are.

However, historically, a simplified view of multi-particle systems, notably of gases and vapors, proved extremely fruitful in developing a sufficiently quantitative accounting of the underlying physics. This view postulated the existence of an equilibrium state of macroscopic samples of diluted gases, in which individual particles move randomly in a given containment, with little or no mutual interactions. The internal state of such "ideal gas" samples could be tested by summary interactions of the gas with the environment beyond the container. It turns out that, at room temperatures and pressures of up to $10^5 Pa$ ($\leq 1\ atm$), many gases with simple particle structure are close to ideal. This category includes the noble gases, as well as most gases in the atmosphere, such as hydrogen, oxygen, and nitrogen.

Molecular Chaos

To summarize briefly the effects of multiple particle interactions, it suffices to note that it only takes a few successive collisions with other particles to deflect a given particle from its initial flight path into random directions. The hard sphere scattering model predicts a random angular distribution already for single

scattering events. In addition, in a collision between equal masses, the collision partners share on average the kinetic energy of relative motion. Energy and momentum are transferred on average from the faster to the slower particle. In such multi-scattering processes, the motion of the gas particles becomes completely chaotic, with an isotropic angular distribution of the velocity $\vec{u}=\{u_x,u_y,u_z\}$ and a chaotic velocity spectrum $f(\vec{u})$.

These rather general observations are sufficient to constrain the chaotic velocity and energy spectra of gas particles to certain classes of functional probability distributions $f(\vec{u})$. Since $f(\vec{u})$ **is a stochastic function (a probability distribution)**, it must be normalized, or at least normalizable:

$$\int d^3\vec{u}\, f(\vec{u}) = \int du_x du_y du_z\, f(u_x,u_y,u_z) = \int du\, u^2 d\Omega\, f(u,\theta,\phi) = 1 \quad (1)$$

The integral limits in Equ.(1) include all (allowed) velocities. Rigorously, although the various functions *f* in Equ. (1) represent the same physical relation, they are different mathematical relations. Given such a probability function, one can calculate the mean (average) velocity $\langle\vec{u}\rangle$ as,

$$\langle\vec{u}\rangle = \int d^3\vec{u}\left[\vec{u}\cdot f(\vec{u})\right] \quad (2)$$

and the average speed as

$$\langle u\rangle = \langle|\vec{u}|\rangle = \int d^3\vec{u}\left[|\vec{u}|\cdot f(\vec{u})\right] \quad (3)$$

The variance of the velocity distribution is defined as the second (central) moment:

$$\sigma_u^2 = \left\langle \vec{u}^2 \right\rangle - \left\langle \vec{u} \right\rangle^2 = \int d^3\vec{u} \left[\vec{u} - \left\langle \vec{u} \right\rangle \right]^2 \cdot f\left(\vec{u}\right) \qquad (4)$$

One can now use symmetry arguments to constrain the possible choices for function $f\left(\vec{u}\right)$.

Because of the isotropy of the velocity distribution, $f\left(\vec{u}\right)$ ***cannot actually depend on the direction of the velocity vector***. It must be an even function in velocity space:

$$f\left(\vec{u}\right) = f\left(-\vec{u}\right) \qquad (5)$$

It can therefore depend only on the absolute value (the speed) or the square of the velocity, i.e., this distribution has the form In particular, one has to require that

$$f\left(\vec{u}\right) = f\left(\left|\vec{u}\right|\right) = f\left(\vec{u}^2\right) \qquad (6)$$

Specifically, one has to require that there are no differences in the probabilities for the three velocity components u_x, u_y and u_z,

$$f(u_x^2) = f(u_y^2) = f(u_z^2) \qquad (7)$$

and, since $u^2 = u_x^2 + u_y^2 + u_z^2$,

$$f(u^2) = f(u_x^2 + u_y^2 + u_z^2) = f(u_x^2) \cdot f(u_y^2) \cdot f(u_z^2) \qquad (8)$$

The relation (8) indicates a peculiar dependence of the probability density *f* on its variables. The functional value of a sum of variables equals the product of the functional values for each term in the sum. In fact, there is only one mathematical function that

shows this behavior: The probability function has to be an exponential in u^2,

$$\boxed{f(u^2)=C\cdot e^{-au^2}} \tag{9}$$

where ***a*** and ***C*** are constants yet to be determined.

The ***constant a has to be a positive number***, a negative number would make the probability become indefinitely large for large velocities, which makes physically no sense. As a probability (or probability density), $f\left(\vec{u}^2\right)$ ***must be normalizable***,

$$1=\int_{-\infty}^{+\infty} du\, f(u^2)=C\cdot\int_{-\infty}^{+\infty} du e^{-au^2} \tag{10}$$

This condition determines the normalization constant to $\boldsymbol{C=\sqrt{(a/\pi)}}$. The constant ***a*** can also be determined, at least it can be related to the mean kinetic energy for each degree of freedom:

$$\left\langle \varepsilon_x \right\rangle=\frac{m}{2}\overline{u_x^2}=\frac{m}{2}\sqrt{\frac{a}{\pi}}\cdot\int_{-\infty}^{+\infty} du_x\cdot u_x^2\cdot e^{-au_x^2} \tag{11}$$

Because of the equality of the average speeds in all directions (Equ.(7)), one obtains similar expressions for

$$\left\langle \varepsilon_y \right\rangle=\left\langle \varepsilon_z \right\rangle=\left\langle \varepsilon_x \right\rangle=\frac{1}{3}\left\langle \varepsilon \right\rangle \tag{12}$$

The integrand in (11) is an ***even function of u_x*** and, hence, the value of the integral is twice that taken along only the positive ***u_x***-axis:

$$\int_{-\infty}^{+\infty} du_x\, u_x^2\, e^{-au_x^2} = 2\cdot\int_{0}^{+\infty} du_x\, u_x^2\, e^{-au_x^2} = \frac{1}{2a}\sqrt{\frac{\pi}{a}} \qquad (13)$$

Combining Equs. (10) and (11), one obtains

$$\langle \varepsilon_x \rangle = \frac{m}{2}\sqrt{\frac{a}{\pi}}\cdot\frac{1}{2a}\sqrt{\frac{\pi}{a}} = \frac{m}{4a} \qquad (14)$$

This determines $a = \dfrac{m}{4\langle \varepsilon_x \rangle}$ and

$$\boxed{f(u_x) = C\cdot e^{-au_x^2} = \sqrt{\frac{m}{4\pi\langle \varepsilon_x \rangle}}\cdot exp\left\{-\frac{m}{4\langle \varepsilon_x \rangle}u_x^2\right\}} \qquad (15)$$

This is a remarkable result of the above symmetry considerations. The velocity distribution (in x) is a Gaussian with a variance of

$$\sigma_{u_x}^2 = 2\langle \varepsilon_x \rangle / m \qquad (16)$$

Similarly, one obtains Gaussians for the u_y and u_z velocity distributions with identical variances. Because of Equ. (12),

$$\sigma_{u_x}^2 = \sigma_{uy}^2 = \sigma_{uz}^2 = \frac{2}{3m}\langle \varepsilon \rangle \qquad \mathbf{(17)}$$

Phenomenologically, one associates the average energy of gas particles (or of constituents of other media) with an equilibrium temperature or non-equilibrium temperature-like parameter T. The higher the average kinetic energy of the

particles, the higher the temperature. Specifically, one measures for each degree of freedom the same mean energy content,

$$\langle \varepsilon_x \rangle = \langle \varepsilon_y \rangle = \langle \varepsilon_z \rangle = \frac{1}{2} k_B \cdot T \tag{18}$$

Here k_B is the Boltzmann constant,

$$\boldsymbol{k_B = R/L = 1.381 \cdot 10^{-23} J/K} \tag{19}$$

This then yields an overall velocity distribution of the gas particles,

$$f(u_x) = C \cdot e^{-au_x^2} = \sqrt{\frac{m}{2\pi k_B T}} \cdot exp\left\{ -\frac{mu_x^2}{2k_B T} \right\} \tag{20}$$

for one velocity component. Then, using Equ. (4), the probability distribution for the total velocity is obtained from Equ. (20) by multiplying three equal terms of the same form, such that

$$f(\vec{u}) = \tilde{f}(u^2) = \left(\frac{m}{2\pi k_B T} \right)^{3/2} \cdot exp\left\{ -\frac{mu^2}{2k_B T} \right\} \tag{21}$$

This is the famous ***Maxwell-Boltzmann velocity distribution***, mathematically a Gaussian function. It has the essential analytical structure of the probability *P(u)* to find the value of ***any*** stochastic single-particle ***variable u*** realized in a statistical (chaotic) system characterized by a temperature *T*: For example, if the energy associated with the value of the variable is calculated as ε (here, the particle kinetic energy) $\varepsilon(u)=(m/2)u^2$), then this probability is given by the ***Boltzmann factor***

$$P(u) \propto exp\left\{-\frac{\varepsilon(u)}{k_B T}\right\} \tag{22}$$

More precisely, the function ***f*** is not directly a probability but a ***probability density***:

$$f(u_x)=\frac{dP(u_x)}{du_x} \tag{23}$$

$$f(\vec{u})=\frac{dP(u_x)}{d^3\vec{u}} \tag{24}$$

In order to obtain a dimensionless, normalized probability ΔP, one has to multiply $f(u_x)$ by a velocity difference Δu_x or $f(\vec{u})$ by a *3D*-volume element $d^3\vec{u}$.

As an example of the use of the velocity distribution, one may calculate the average *x*-velocity u_x of the particles (mass *m*) in a gas at temperature *T.* From Equ. (20), one gets

$$\langle u_x \rangle = \sqrt{\frac{m}{2\pi k_B T}} \int_{-\infty}^{+\infty} du_x' u_x' \cdot exp\left\{-\frac{m u_x'^2}{2k_B T}\right\} = 0 \tag{25}$$

This follows, because the integrand is an ***odd function of u_x'***, hence, the negative contributions are canceled by the positive ones. Physically, this result means that ***neither the positive nor the negative x direction is preferred***, as should be the case for truly random motion. On the other hand, the average ***speed is obviously non-zero,*** $|u_x| \geq 0$, mathematically because

$$\langle |u_x| \rangle = \sqrt{\frac{m}{2\pi k_B T}} \int_{-\infty}^{+\infty} du'_x \, |u'_x| \cdot exp\left\{ -\frac{m u'^2_x}{2k_B T} \right\} = \\ = 2\sqrt{\frac{m}{2\pi k_B T}} \int_{0}^{+\infty} du'_x u'_x \cdot exp\left\{ -\frac{m u'^2_x}{2k_B T} \right\} = \tag{26}$$

With a variable transformation $v = u_x' \cdot \sqrt{(m/2k_BT)}$, one obtains an integral solved in any of the familiar integral tables:

$$\langle |u_x| \rangle = \frac{2}{\sqrt{\pi}} \sqrt{\frac{2k_B T}{m}} \int_0^{\infty} dv \cdot v \cdot exp\{-v^2\} = \sqrt{\frac{2k_B T}{m\pi}} \tag{27}$$

Similarly, one can calculate the average of u^2, and the ***mean-square velocity*** $\sqrt{\langle u^2 \rangle}$. Because of Equ.(25), this velocity is equal to the ***variance*** $\sigma^2_{u_x}$ ***in the velocity distribution***

$$\sigma^2_{u_x} = \langle u^2_x \rangle - \langle u_x \rangle^2 = \frac{2}{\sqrt{\pi}} \frac{2k_B T}{m} \int_0^{\infty} dv \cdot v^2 \cdot exp\{-v^2\} = \frac{k_B T}{m} \tag{40}$$

which is equal the average kinetic energy (Equ. (18)31) for motion in x direction, divided by m/2. Note that $\langle |u| \rangle^2 \neq \langle u \rangle^2$. Hence, the velocity distribution of Equ. (21) is a Gaussian with a variance equal to the quantity $k_BT/m = 2\langle \varepsilon_x \rangle / m$, i.e., ***the fluctuation in the velocity determined by the average in the kinetic energy, i.e., by the temperature T.***

It is also straight-forward to derive the associated Maxwell-Boltzmann energy distribution, by transforming Equ. (21) to particle ***kinetic energy*** $\varepsilon = (m/2)u^2$. One notices that the probability $dP(\vec{u})$ to find particles with velocities between u and $u+du$ in the

solid-angle element $d\Omega$ is the same as that, $dP(\varepsilon)$, for particles of the ***corresponding energies*** between $\varepsilon=(m/2)u^2$ and $\varepsilon + d\varepsilon$ in the same element $d\Omega$. Since $d\varepsilon = mu\,du$ and $u^2du=(u/m)\,d\varepsilon$, and using the ***chain rule of differentiation***, one has

$$\frac{dP(\vec{u})}{u^2 du d\Omega} = \frac{d^2P(\varepsilon)}{u^2 d\varepsilon d\Omega}\frac{d\varepsilon}{du} = \frac{d^2P(\varepsilon)}{d\varepsilon d\Omega}\frac{m}{u} \qquad (28)$$

From this equation and Equs. (21)-(24), one obtains the differential

Maxwell-Boltzmann kinetic-energy spectrum

$$\frac{dP(\varepsilon)}{d\varepsilon d\Omega} = \frac{u}{m}\frac{dP(\vec{u})}{d^3\vec{u}} = \sqrt{2}\left(\frac{1}{2\pi k_B T}\right)^{3/2}\cdot\sqrt{\varepsilon}\cdot e^{-\frac{\varepsilon}{k_B T}} \qquad (29)$$

Note that this spectrum does not depend on the particle species at all! It is the same for particles of any mass. Because there is no angle dependence of the energy spectrum, the angle-integrated spectrum is equal to that of Equ. (28), just scaled up by a factor of 4π, since $\int d\Omega = 4\pi$ is the total solid angle (see tutorial),

$$\boxed{\frac{dP(\varepsilon)}{d\varepsilon} = 4\pi\frac{u}{m}\frac{dP(\vec{u})}{d^3\vec{u}} = 2\left(\frac{\pi}{k_B T}\right)^{3/2}\sqrt{\varepsilon}\cdot e^{-\frac{\varepsilon}{k_B T}}} \qquad (30)$$

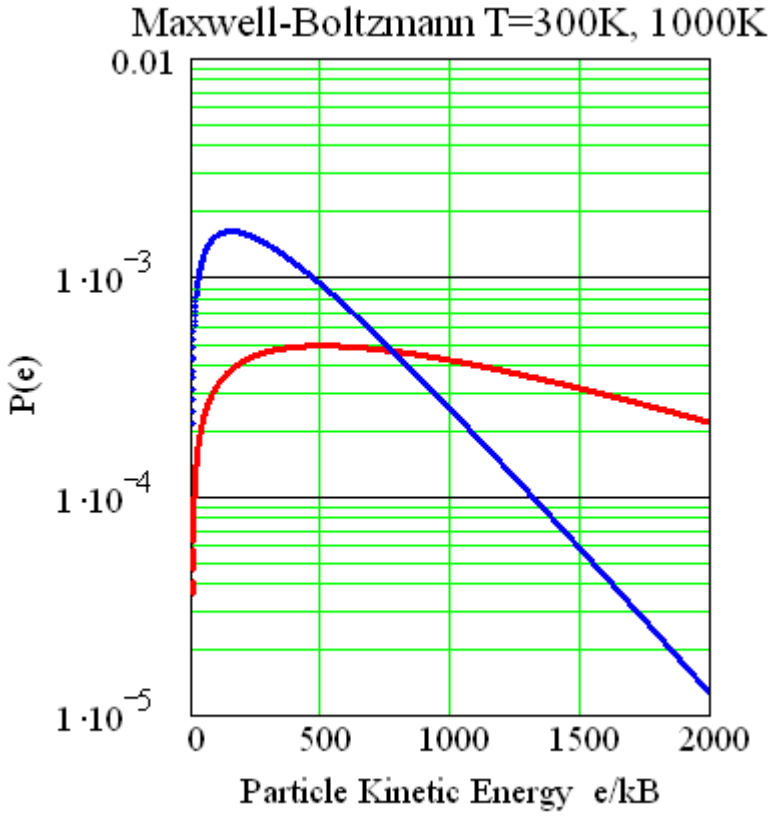

Figure 1: Maxwell-Boltzmann energy distribution of a gas in molecular chaos, for temperature of *T*=300 (blue) and *T*=1000K (red).

The figure on the left illustrates, on a logarithmic scale, the shapes of ***Maxwell-Boltzmann*** energy distributions for *generic* particles in a gas at the two very different temperatures of $T = 300K$ and $T = 1000K$ calculated with a Mathcad code.

Plotted in the figure are the probabilities for finding in the gas a molecule with an energy of ε which is given in temperature equivalent units of $1/k_B$. ***Typical absolute energies are of the order of 10^{-19}J per particle***.

The approximately exponential character of the random (chaotic) velocity distribution is clearly visible on the logarithmic scale. Except for the square-root ($\sqrt{\varepsilon}$) dependence at low energies, the distributions have an exponential character reflecting the temperature,

$$\lim_{\varepsilon\to\infty}\frac{d}{d\varepsilon}\ell n\left(\frac{dP(\varepsilon)}{d\varepsilon}\right)=-\frac{1}{k_BT} \qquad (31)$$

This suggests a simple and ***elegant method to measure the temperature*** of a gas. Clearly, the *T = 1000 K* spectrum is much harder ("*shallower*") than that for the lower temperature, demonstrating the important fact that ***the logarithmic slope of the energy spectrum is a direct measure of the temperature of the gas***. However, caution should be exercised in practical cases, where the limit of $\varepsilon \to \infty$ cannot be taken, because the spectra contain no significant intensity at high energies.

The single-particle kinetic energies are typically only of the order of 10^{-19} *J*. When plotted in units of J^{-1}, the probabilities have extremely small magnitudes. Hence, one often quotes kinetic energies and related variables for moles of particles ($N = 6 \cdot 10^{23}$ particles). For an *N*-particle system, one has to multiply the expressions (e.g., Equ. (30)) with *N,* in order to find the number of particles at a given energy.

The ***analytical*** Maxwell-Boltzmann ***formula*** (Equ. (30)) derived above suggest a smooth behavior of the associated probabilities.
However, a ***finite number of particles can obviously not have a smooth behavior,*** as far as actually observed velocity and energy distributions are concerned. These will show ***statistical fluctuations*** about the general shapes predicted by theory, with fluctuations determined by the number of particles. A way of illustrating such statistical distribution is by ***sampling*** these formulas by Monte Carlo methods.

The results of such a simulation are shown in the figure below (Fig.2) representing "snapshots" of the kinetic-energy distributions for ideal gases of *1000* particles at *T=300K* (left) and at *T=500K* (right) (BOLTZMANN_MONTECARLO-01.mcd), illustrating ***microstates of the system***. Here the kinetic energies of the

particles are given in multiples of the Boltzmann constant k_B, i.e., as ε/k_B. These ratios have units of *K(Kelvin)* represent temperatures. The number *n* simply numbers the gas particles.

From Fig. 2 below, one observes that the particles are more concentrated at lower energies, near the bottom of the "scatter plot". Towards higher energies, the density of particles decreases exponentially, on average it is given by Equ. 30. Nevertheless, there are a few particles present in the spectrum with very high

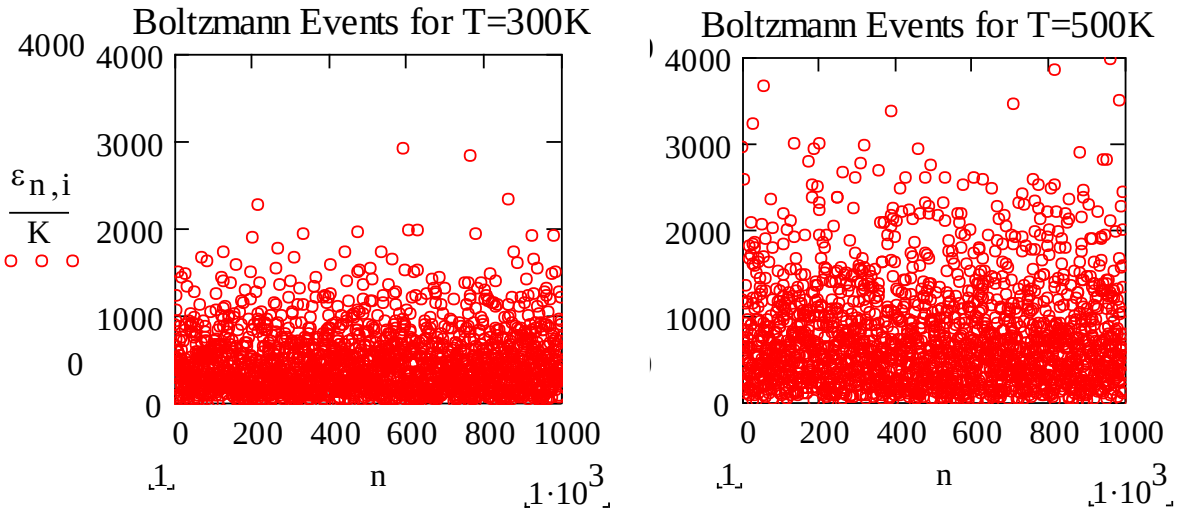

Figure 2: Snapshots of Maxwell-Boltzmann energy distributions for 1000 gas particles at T=300K (left) and T= 500K (right).

energies. For the higher temperature (*T=500K*) shown in the figure on the right, the distribution of particle energies is broader and somewhat less dense, and the density changes less rapidly with energy, than at *T=300K*.

Because of the continuous scattering and re-scattering of the particle, the distributions of all variables change dynamically in time, they fluctuate about the thermodynamic average. This effect is illustrated in an animation (***click on link to view***) showing the time-dependent fluctuations in this energy distribution for *T = 300K.* For this temperature, the Fig. 3 illustrates how the two first

moments ***of the distribution*** in energies, average energy (©ε^{TM} = εaver) and the variance (σ_ε^2 = εvar) of the particle kinetic energies change with time, proceeding here with snapshot number *i*. Note that the ordinate scale is double-valued, the units are *K* for the average energy and K^2 for the variance.

In analogy to the earlier discussion of the average and variance

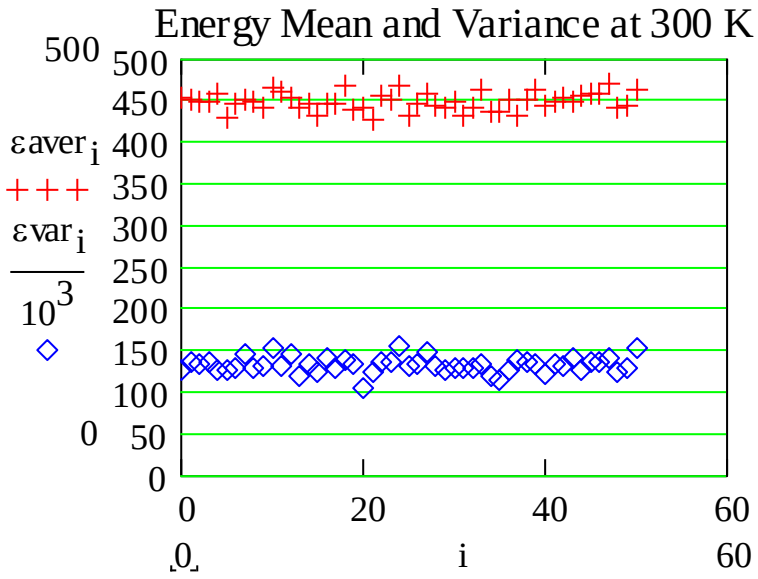

Figure 3: Average energy/k_B and variance/k_B^2 of a Maxwell-Boltzmann energy distribution for a sample of 100 gas particles viewed at 50 different times.

(*1st* and *2nd* moment) of the velocity (probability) distribution, the average kinetic energy and its spread are defined in terms of the distribution function of Equ. (30).

As a concluding remark to this section about molecular chaos, it is pointed out that only weak assumptions have been made about random direction and distribution of the energy among a specific set of observables (here translational particle velocities). While it is natural to associate such a situation with a complete

thermodynamic equilibrium of all degrees of freedom of a given system, this constraint is not necessary. The general conclusions of this section are valid also for subsystems that behave chaotically ("local equilibrium") but do not share their energy content with the entire system and all of its degrees of freedom. For example, the particles in a local hot spot of a large ensemble of particles can behave like such a subsystem that, over longer time periods, will dissipate their higher energy content over the larger system by a diffusion-like transport process.

Equation of State of Ideal Gases

As explained in other sections, the cumulative effect of multiple interactions of the constituents of a medium, for example the molecular collisions in a gas, is to spread the available energy evenly over all accessible degrees of freedom. Degrees of freedom for individual particles include translation motion along x, y, and z spatial degrees of freedom and associated velocity components, which are all **stochastic variables**. Such an even distribution of the total available energy only implies that the average energy carried by each degree of freedom is the same ($1/2k_BT$), not that all constituents or instants have the same energy. **All stochastic variables show statistical (thermal) fluctuations about their mean values. They have a probability distribution.**

Mean values or averages of observables of a complex, multi-dimensional (multi-particle) system are called **macroscopic variables (state functions),** because these quantities is what can be observed in a macroscopic measurement involving matter quantities of the order of significant fractions of a mole or more. An example is the mean kinetic energy or pressure of an ensemble of, perhaps, 10^{23} particles. The **Equation of State** (EOS) of a system relates its fundamental macroscopic variables to one another. The EOS can be deduced from the behavior of such systems upon external influences, energy transfer, compression, dilution, etc.

At this point it is useful to make a detour to experiment to recall how a minimal set of macroscopic variables can be defined for simple systems such as **very dilute chaotic gases of structure less point particles enclosed in containers**. Such gases are also called "ideal" or interaction-free. They are realized in nature only in approximation but are used as conceptual tools.

In general, energy can be transferred to any (generic) system/object in a state of relatively low energy, e.g., in its ground state, either by mechanical compression, by exposure to flames or various types of radiation, by running electrical currents (sparks) through it, and by other means. Several macroscopically observable phenomena typically occur in response to such excitation:

1. The object "heats" up, i.e., it acquires an increased "temperature" *T*.
2. The system expands and potentially changes state (deforms, melts, sublimates, boils).
3. Eventually, at long times, it reaches a steady state termed "thermal equilibrium."
4. Several objects in close mechanical ("touching") contact acquire the same temperature.

Operationally, the concept of a temperature is defined in terms of observable and reproducible expansion effects of gases, liquids, and solids. The **Celsius** temperature scale (0^oC) is calibrated at 0^oC and 100^oC using the solidification and vaporization of liquid water, respectively.

With an expansion coefficient α, one observes experimentally a temperature dependence of the volume V of a fixed amount of substance of the form,

$$V(T)=V(0)\cdot\left[1+\alpha\cdot T\right] \qquad (32)$$

Typical values of expansion coefficients for metals are $\alpha(Cu)=1.6\cdot10^{-5}/^0C$ and $\alpha(Zn)=2.9\cdot10^{-5}/^0C$. For liquids, the corresponding coefficients are larger, e.g., $\alpha(H_2O)=4.3\cdot10^{-4}/^0C$, α(petrol)$=1.0\cdot10^{-3}/^0C$, α(ether)$=1.6\cdot10^{-3}/^0C$. This behavior suggests stronger cohesive (atomic or molecular) forces at work in metals

than in liquids. The trend continues with gases: For many dilute gases at fixed pressure (*p=const.*) the expansion coefficient is essentially equal, α(dilute gases)=$3.66\cdot10^{-3}/^0$C≈$1/273^0$C. The latter observation is the content of the **Law by Gay-Lussac**. The universal gas expansion coefficient suggests a more convenient **Kelvin** (absolute) temperature scale (^{0}K =^{0}C+273.15), which has its zero at -273^0C. Then, Equ. (32) can be rewritten as

$$V(T)=V(0^0C)\cdot\left[1+\alpha\cdot T\right]=\frac{V(0^0C)}{273^0C}\cdot\left[273^0C+T\right] \qquad (33)$$

Similarly, if dilute gases are enclosed in a fixed volume V and heated, their pressure increases according to,

$$P(T)=P(0)\cdot\left[1+\alpha\cdot T\right] \qquad (34)$$

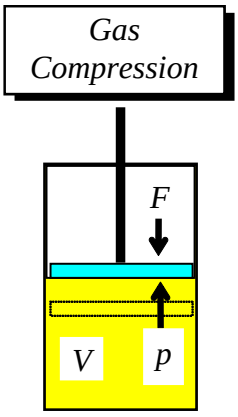

Figure 4: Testing Boyle's Law with gas filled cylinder and a movable piston.

On the other hand, a very important empirical gas law is named ***Boyle's Law*** after the English chemist ***Robert Boyle***. He found that, for a given amount *n* (number of moles) of gas, and at fixed temperature *T*, the ***internal gas pressure p increases when the gas is compressed by the action of an external force F***, i.e., when the gas volume *V is* decreased, and *vice versa* (see Fig. 4). It requires an external force *F* against the internal gas pressure *p*, in magnitude equal to the product of pressure and area on which the force is applied, to affect a compression. The experimental correlation *p(V)* was well described by a ***hyperbolic function***

$$P(V)\propto 1/V \quad \text{or} \quad P\cdot V=const(n,T) \qquad (35)$$

If both, *p* and *V* are allowed to vary at fixed temperature, one finds

$$P(T)\cdot V(T)=P(0)\cdot V(0)\cdot\left[1+\alpha\cdot T\right] \qquad (36)$$

or

$$\boxed{P\cdot V=n\cdot R\cdot T=N\cdot k_B\cdot T\rightarrow P=\rho\cdot k_B\cdot T} \qquad (37)$$

In Equ. (37), *n* is the number of gas moles in *V*, $\rho=N/V$ their density, and ***R = 8.31451 J/(K∃□mole)*** is the universal **Gas Constant**. The equivalent expression in Equ. (37) involving the number of particles *N*, has as proportionality coefficient the **Boltzmann Constant k_B**.

Equation (37) is the Ideal-Gas Equation of State (EOS). It describes the **macroscopic equilibrium** state of a dilute gas volume completely in terms of the state variables ("functions") pressure, volume, and temperature. At the absolute zero of the Kelvin temperature scale, neither pressure nor volume of the gas are measureable, *p=0, V=0*.

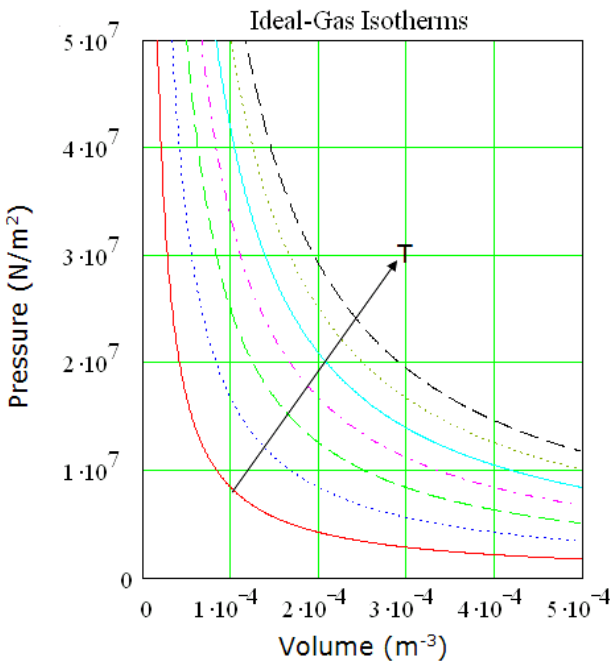

Figure 5: Ideal-gas isotherms for various temperatures *T*.

Figure 15 shows as examples of the ideal gas **EOS** the isotherms (T=const.) in a plot of pressure vs. volume, *V*.

The task is now to understand the structure of this EOS (Equ. (37) in terms of the very simple microscopic model of a dilute

"ideal" gas of weakly or non-interacting, structure-less particles (atoms or molecules). In this approximation, particles move randomly inside a container, **explicit particle-particle interactions are neglected,** but their **randomizing effect is implicitly assumed.** In addition, **elastic collisions of the particles with the walls of the container are considered.**

Consider first a single gas particle of mass *m* and initial momentum $\vec{p}_i$ in a rectangular container with rigid walls, shown on the left in cross-sectional view. Let a coordinate system **{x,y,z}** be aligned with the edges of the container. This geometry facilitates the following calculation but does not restrict the generality of the conclusions.

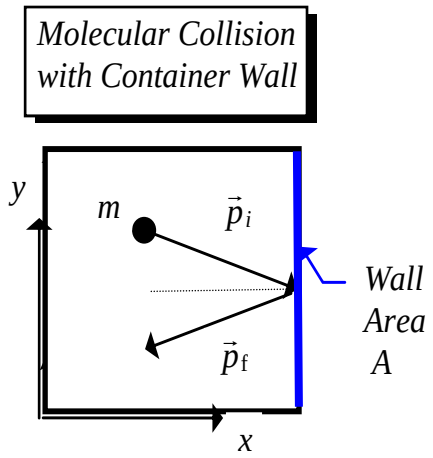

Figure 6: Momentum reversal in wall collisions

The particle under consideration will eventually collide with one of the container walls, e.g., the one on the right, which is assumed to be parallel to the y-z plane. The collision with the rigid wall is assumed to be **elastic**, i.e., essentially **no energy is lost** by the particle. This would be exactly true only, if the mass (***M***) of the wall were infinitely large, such that a collision with a gas particle would impart very little energy, namely $E_{wall} = q^2/(2M) \approx 0$, for any **momentum *q* transferred** to the wall.

For the present discussion, it suffices to assume that the mass M of the wall is very large compared to the mass m of a gas particle ($M \gg m$). Then, the particle is reflected almost perfectly from the wall. That is, its momentum components parallel to the wall, p_y and p_z, are not changed in the collision, but the component perpendicular to it, p_x, is reversed in direction, i.e., it changes its sign but not its magnitude $|p_x|$:

$$\vec{p}_i = \begin{pmatrix} p_x \\ p_y \\ p_z \end{pmatrix} \quad \rightarrow \quad \vec{p}_f = \begin{pmatrix} -p_x \\ p_y \\ p_z \end{pmatrix} \qquad (38)$$

before *after*

In every collision, there is ***conservation of linear momenta***, i.e., the sum of all momenta remains constant. Then, the wall must have received the difference in the momenta of the particle before and after the collision. This must always be true, even though the mass of the wall is assumed to be very large. This momentum transfer to the wall is simply equal to

$$\vec{q} = \vec{p}_i - \vec{p}_f = \begin{pmatrix} 2p_x \\ 0 \\ 0 \end{pmatrix} \qquad (39)$$

This means that the container wall experiences a "kick" in the *x* direction. This kick can be viewed as a ***force δF_x, acting on the wall during the short time Δt*** of the collision. Because of Newton's Law, the relation between momentum transfer and force is given by

$$\delta F_x \cdot \Delta t \; = \; q_x = 2p_x \qquad (40)$$

δF_x is the force that the container wall "feels" during the time Δt, from the ***effect of a single particle*** colliding with it.

However, presumably there are many particles in the gas container, some of which collide with the wall on the right, some collide with one of the other walls. The next question is: ***How many***

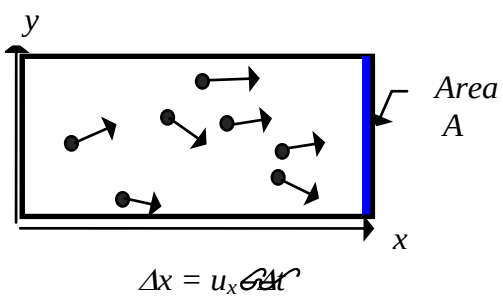

Figure 7: Collision layer in front of wall.

particles collide with the wall during the same (small) time interval Δt?

The answer is simple and can be obtained by counting the number of particles in the **collision layer** moving towards the wall: If a particle has a velocity component in positive *x* direction, i.e., $u_x = p_x/m > 0$, the particle moves to the right and will eventually hit the right wall, those with $u_x < 0$ will hit the wall on the left. If, by assumption, the ***motion of the gas particles is truly random***, 1/2 of the particles will have $u_x < 0$, the other 1/2 will have $u_x > 0$. If there are *N* particles in the container, then *N/2* will *eventually* collide with the wall in question.

However, only those particles that are close enough to the wall will actually ***hit it during Δt***. Only those that are ***closer than*** $\Delta x = |u_x| \exists \Delta t$ ***and have*** $u_x > 0$ will do so. This implies that ***all particles in the collision volume*** $\Delta V = A \exists u_x \exists \Delta t$ ***with*** $u_x > 0$ ***will impinge on the wall***. With a ***particle density of*** $\rho = N/V$, one calculates that

$$\Delta N_+ = (1/2)\rho \cdot \Delta V = (1/2) N \cdot A \cdot u_x \cdot \Delta t / V \qquad (41)$$

particles impinge on the wall within the time interval *Δt,* each transferring a momentum $q_x = 2p_x$ to the wall. The total momentum transfer during *Δt* is then given by

$$\Delta F_x \cdot \Delta t = (\Delta N_+ \cdot \delta F_x) \cdot \Delta t = \Delta N_+ \cdot (2p_x) = N \cdot A \cdot m\, u_x^2 \cdot \Delta t / V \quad (42)$$

Therefore, the pressure[1] $\boldsymbol{P_x}$ on the wall, defined as ***force*** ΔF_x ***per area A***, can be written as

$$\boldsymbol{P_x} = \boldsymbol{P} = \Delta F_x / A = N\, m\, u_x^2 / V \qquad (43)$$

or

$$P \cdot V = N \cdot m \cdot \overline{u_x^2} \qquad (44)$$

Realizing that the particles may not all have the same velocity, in Equ. (44) the quantity ***u_x^2 has been replaced by its average over many collisions,*** $\overline{u_x^2}$.

A similar calculation can be done for any other wall, taking into consideration also the other components, u_y and u_z, of the gas particles. If, as assumed, the motion is truly random, then there is no reason, why the average of the velocity u_x in x direction*, or its square,* should be any different from those in other directions. Therefore, it is justified to take

$$\overline{u_x^2} = \overline{u_y^2} = \overline{u_z^2} = (1/3)\overline{u^2} \qquad (45)$$

where the ***speed*** of the particles is defined as

$$u = |\vec{u}| = \sqrt{u^2} = \sqrt{u_x^2 + u_y^2 + u_z^2} \qquad (46)$$

Then, Equ. (44) can be transformed into

$$P \cdot V = N \cdot (1/3) m \cdot \overline{u^2} \qquad (47)$$

[1] When, like here, there is possible confusion between pressure and momentum, pressure will be indicated by a capital letter *P*.

which is now independent of coordinate system.
Since the kinetic energy of a gas particle is equal to $\varepsilon=(1/2)mu^2$ relation (47) can be rewritten as

$$P \cdot V = N \cdot (2/3)\bar{\varepsilon} \qquad (48)$$

Equation (48) makes good sense, because it relates a quantity like the ***total energy content*** **[*p·V*=(*force/area*)· *area·distance*]** *of* the gas to a product of average energy per particle ($\bar{\varepsilon}$) and the number of particles (*N*) in the gas volume. The volume *V* and hence the product *p·V*, must scale with the number of particles. It is said to be an **extensive variable**. Because of that fact, *PV* must scale as $\boldsymbol{P \cdot V \propto N^1}$, and no other power of *N* must appear in this expression (Equ. (48)).

In other words, the average ***specific kinetic energy*** $\bar{\varepsilon}$ is seen to determine the magnitude of the total ***energy content*** per particle, *P·V/N*, as is plausible. This ***average specific energy*** $\bar{\varepsilon}$ ***naturally depends only on the heat content of the gas, which is determined by the temperature T***. What remains to be explained is the factor (2/3) in Equ. 61. The present phenomenological treatment does not explain this factor, it only provides the structure of the *EOS*. However, comparing Equ. (48) with the experimental observation of the ideal-gas law, $p \cdot V = N \cdot k_B \cdot T$, one derives an expression for the ***average kinetic energy of the gas particles***:

$$\bar{\varepsilon} = \frac{3}{2} \cdot k_B T \qquad (49)$$

Furthermore, since the motion of the particles along any of the *x, y,* and *z* ***"degrees of freedom"*** is independent, the average total

energy is equal to the sum of the average energies associated with the individual degrees of freedom,

$$\bar{\varepsilon}_x = \bar{\varepsilon}_y = \bar{\varepsilon}_z = \frac{1}{2} k_B T \tag{50}$$

which is identical to Equ. (18), where this relation had been anticipated. The quantity

$$c = \frac{3}{2} k_B \tag{51}$$

is the specific heat capacity of a particle with only translational degrees of freedom. As will be shown later, one can extend the result of Equ. (51) to all independent degrees of freedom of the system considered and formulate an **Equipartition Law**:

In thermal equilibrium, each degree of freedom has an average energy given by the amount (1/2)k_BT.

One can turn this result around and obtain an illustration of the concepts "temperature" or "heat" energy. The absolute temperature of a system in thermal equilibrium is given by its total internal energy divided by the total heat capacity. Heat energy is distinguished from other types of energy by the fact that it is evenly partitioned (distributed) over all degrees of freedom of the system.

A very obvious and useful application of the *EOS* concerns ***mixtures of different ideal gases*** in the same given volume *V* and at the same temperature *T*. Let the amounts (numbers of moles) of the *A* different gases in this volume be $n_1, n_2,\ldots,n_A$. Ideal gases are so dilute that the ***gas particles do not "feel" the presence of the other particles***, one speaks of an ideal gas of

"interaction-free" particles. Then ***each gas obeys the same EOS*** (Equ. 61), such that each individual, ***partial pressure*** P_i is given by

$$P_i = n_i \cdot R \cdot T/V \qquad (52)$$

Then the total amount of gas is given by $n = \sum_i n_i$, and, according to the *EOS*, one expects for the total pressure *P*:

$$P = nR\frac{T}{V} = \left(\sum_i n_i\right) R\frac{T}{V} = \sum_i \left(n_i R\frac{T}{V}\right) \qquad (53)$$

or

$$P = \sum_i P_i \qquad (54)$$

This is the content of ***Dalton's Law of partial pressures***, saying that the total pressure is simply equal to the sum of the partial pressures of the different gas components, independent of the other properties of the components of the mixture.

The **Equipartition Law** implies that all particles have the ***same average kinetic energies,*** $\overline{\varepsilon(i)}$, which **are dependent only on the common temperature *T* but independent of their masses m_i.** From this statement, one concludes immediately that the velocities must scale with the masses of those particles. Considering, for simplicity, only two different particle types and only the *x* degree of freedom and the associated velocities $u_x(i)$, Equ. 25 can be used to calculate this scaling:

$$\overline{\varepsilon_x(1)} = \frac{m_1}{2}\overline{u_x^2(1)} = \frac{1}{2}k_B T = \overline{\varepsilon_x(2)} = \frac{m_2}{2}\overline{u_x^2(2)} \qquad (55)$$

Therefore, one derives

$$\overline{u_x^2(2)}\Big/\overline{u_x^2(1)}=m_1/m_2 \qquad (56)$$

Obviously, the same arguments can be made for the other degrees of freedom *y* and *z*, saying that the mean-square velocities $\overline{u^2(i)}$ scale inversely proportionally with the masses m_i of the particles, i.e., $\overline{u^2(i)} \propto m_i^{-1}$**.** As will be shown later on, the ***mean velocities*** $\overline{u(i)}$ differ only very little from the ***root-mean-square velocities*** $\langle u \rangle_{rms} = \sqrt{\overline{u^2(i)}}$**.** Hence,

$$\overline{u(i)} \propto m_i^{-1/2} \qquad (57)$$

In thermal equilibrium, heavier particles move more slowly than lighter ones.

This latter principle has important applications for the decomposition of mixtures, e.g., the industrial ***separation of different gas types, of different nuclear isotopes*** of a gas, or the ***differential permeability of membranes*** in biological processes. Here, one uses the scaling of the velocities with the inverse mass to deplete a gas mixture of the more mobile, lighter particles.

The effusion enrichment method uses gas containers with small holes or pores through which particles can escape (effuse) for further processing. The principle is illustrated in the sketch (Fig. 8) showing a container with two gas particle types *i =1,2.* The derivation of the rates of effusion of the particles through the hole in the container is simple, following Equ. (57) with the average *x* velocities of the particles given by $\overline{u_x(i)}$: The number of particles $\Delta N_+(i)$ escaping through the hole of area *A* per unit time Δt is given by

$$\Delta N_+(i) = (1/2)\ \rho_i \cdot \Delta V = (1/2)\ N(i) \cdot A \cdot \overline{u_x(i)}\ \Delta t/V \qquad (58)$$

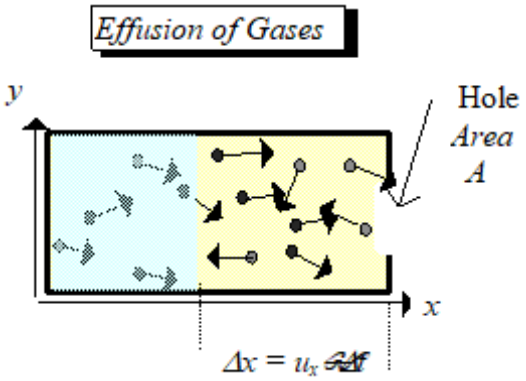

Figure 8: Calculation of the effusion rate using the concept of a collision layer.

where $\rho_i = N(i)/V$ is the ***partial (particle) density*** of component *i.* This is different from the partial ***mass density defined as***

$$\rho_{\mathbf{m}}(i) = \mathbf{m}_i \cdot \rho_i \qquad (59)$$

The effusion rates are then seen to be proportional to the partial densities and to the inverse of the square-root of the particle masses:

$$R_{eff}(i) = \frac{\Delta N_+(i)}{\Delta t} \propto \rho_i \cdot \bar{u}_x(i) \propto \frac{\rho_i}{\sqrt{m_i}} \qquad (60)$$

Finite size and interaction effects: Real Gases

In the above discussion of dilute gases, it was assumed that the finite size, e.g., the radius *R* of the gas particles could be neglected compared to their *mean free path length*, which is a measure of the strength and range of interactions that actually take place between particles. It is simply assumed that particles never come close enough to experience these interactions. This implies that one deals essentially with (unrealistic) point particles.

However, already at normal densities and temperatures, the validity of this assumption is not guaranteed for all gases. It has already been pointed out that at room temperatures and above, interactions between gas particles are essentially governed by the repulsive core of the Lennard-Jones particle interaction potential. This hard core is impenetrable and is simulated approximately by the hard-sphere (hs) contact interactions of macroscopic billiard balls. Ensembles of such hard spheres should behave approximately like chaotic gases because of the randomness of hs scattering. It turns out that the finite volume of the gas particles does not change this behavior of random scattering.

To assess the possible effect on experimental observables, assume spherical gas particles of radius *R* and individual volume $\upsilon = (4\pi/3)R^3$ in a container of volume V. As seen from Fig. 9, the volume ΔV that is not available for a particle in proximity to another has twice the radius of the particle and is 2^3 times the specific volume, $\Delta V = 8 \cdot \upsilon$. Therefore, to account for this inaccessible volume, the ***EOS should refer to an effective volume V_{eff},*** which is smaller than the nominal container volume *V* by an amount corresponding to the finite-size effect for all *N* gas particles:

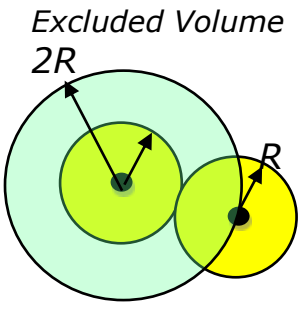

Figure 9: Volume excluded in hard-sphere interactions.

$$V \to V_{eff} = V - 8 \cdot N \cdot \upsilon = V \cdot \left(1 - 8 \cdot \rho \cdot \upsilon\right) < V \tag{61}$$

Alternatively, one can say that the effective density ρ_{eff} is larger than that calculated from the number of particles (N) in a container of nominal volume V. The effective gas density is then

$$\begin{aligned} \rho_{eff} &= \frac{N}{V_{eff}} = \frac{N}{1} \frac{1}{\left(V - 8 \cdot N \cdot \upsilon\right)} \\ \rho_{eff} &= \frac{N}{V} \frac{1}{\left(1 - 8 \cdot \rho \cdot \upsilon\right)} = \frac{\rho}{\left(1 - 8 \cdot \rho \cdot \upsilon\right)} > \rho \end{aligned} \tag{62}$$

The effect is somewhat (50%) smaller at distances of one monolayer from the container walls, since here the gas particles have collision partners only on one side. In any case, because of the excluded "eigen" volume of the particles in a chaotic gas, the pressure is no longer proportional to the density ρ, unlike in Equ. (37) , the "ideal gas" EOS.

The attractive part of the Lennard-Jones interaction has an effect only at relatively low particle energies. Here, the ***L-J*** attraction retards the motion of the particles, since for a given amount of *total* energy per particle supplied from the outside ($1/2k_BT$ per *d.o.f*), the *kinetic* energy is smaller by the amount of (binding) potential energy the particles need to overcome. Hence, the ***actual pressure of a real gas at a given temperature T is smaller than for an interaction free, ideal gas***. The corresponding ideal gas pressure has to be augmented by a differential pressure ΔP, which should depend on the probability that two particles meet within the gas:

$$\Delta P \propto \rho^2 \quad \rightarrow \quad \Delta P \approx -a \cdot \frac{N^2}{V^2} \tag{63}$$

Here, the proportionality factor has been chosen as ***a* > 0** for convenience. As a result, the actual pressure P_{meas} measured for an actual gas will be lower than that for a very dilute, ideal gas. If these are the only effects by which real gases differ from ideal gases, one expects an EOS for real gases at normal densities of the approximate structure

$$P_{IG} \cdot V_{eff} = \left(P_{meas} + \Delta P\right) V \left(1 - 8\rho\upsilon\right) = Nk_B T \tag{64}$$

instead of Equ. 50. This is the so-called ***van der Waals*** EOS for real gases. It is written in shorter form as,

$$\left(P + a\left(\frac{N}{V}\right)^2\right) \cdot \left(V - Nb\right) = Nk_B T \tag{78}$$

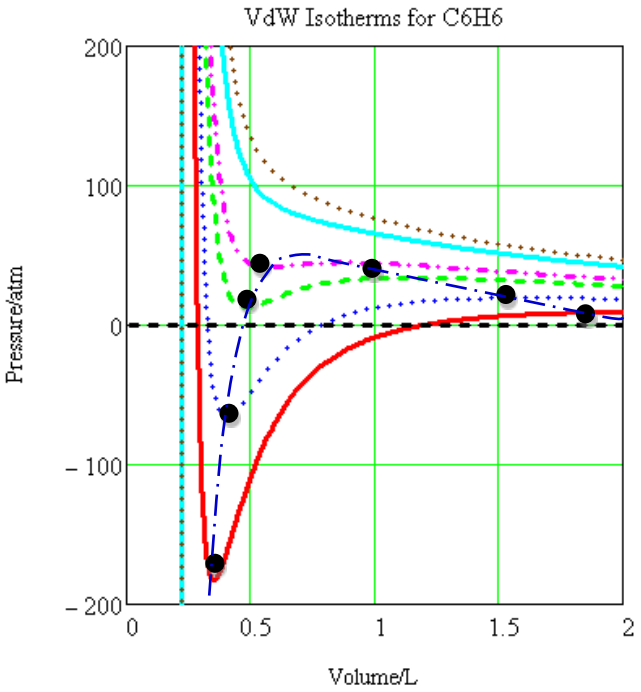

Figure 10: Van der Waals EOS for n=2 moles C_6H_6 for *T*=300, 400, 500, 600, 650, 700K. The dash-dotted curve connecting the solid dots is the spinodal curve.

where the meaning of the parameters *b* and *a* are clear from the above discussion.

As shown in Fig. 10, for temperatures higher than critical temperature (T_{crit}), the ***vdW*** isotherms $P(V)_T$ are monotonic with volume and look very similar to the ideal-gas isotherms of Equ. (37) The gas resist compression by increasing its internal pressure

against the container walls. The higher the temperature, the shallower the curves are, higher the pressure at a given volume. But the behavior of the isotherms changes for temperatures lower than the critical temperature T_{crit} (=304.2K for CO_2). Here, the isotherms become non-monotonic, exhibiting two extrema, a maximum pressure at relatively large volume, and a minimum at smaller volumes. A spinodal curve is included in Fig. 10, marking the points $P(V)_{sp}$.

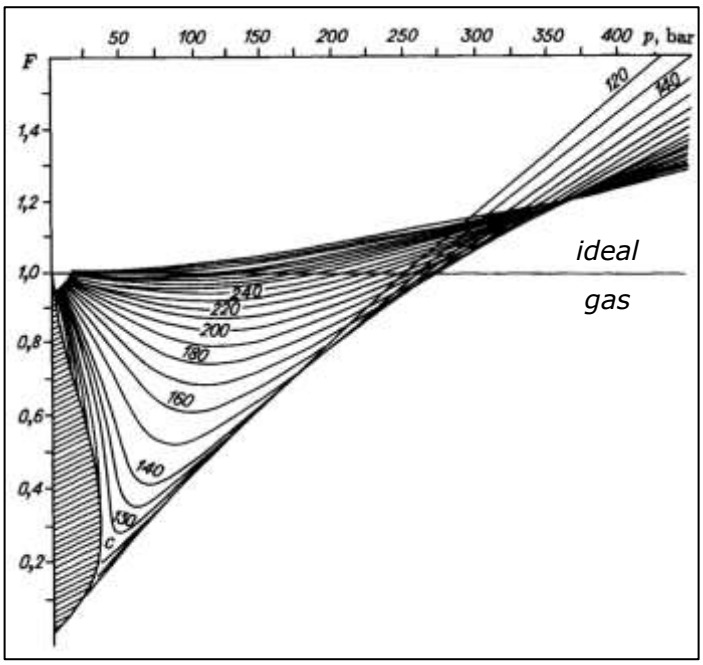

Figure 11: Hougen-Watson compressibility factor *F(p)* for N_2.

Figure 11 illustrates how differently hypothetical vdW and similar model gases (here N_2) are expected to behave as compared to ideal gases. Here the **isothermal compressibility factor**

$$Z(p) = \frac{p \cdot V}{nRT} \qquad (65)$$

is plotted vs. pressure P and different temperatures. Obviously, for an ideal gas, $Z=1$ for all pressures. vdW and other gases modeled on real gases like N_2, start out with $Z=1$ at $p=0$. For larger pressures, they first exhibit smaller compressibility factors ($Z<1$), because they experience inter-particle interaction reducing the kinetic particle energy. At even higher pressures, the repulsive interaction has the opposite effect: Model (and real) gases resist compression more strongly than ideal gases. Mathematically, one can describe the behavior of the compressibility factor in terms of a power series in density or volume ("virial" expansion).

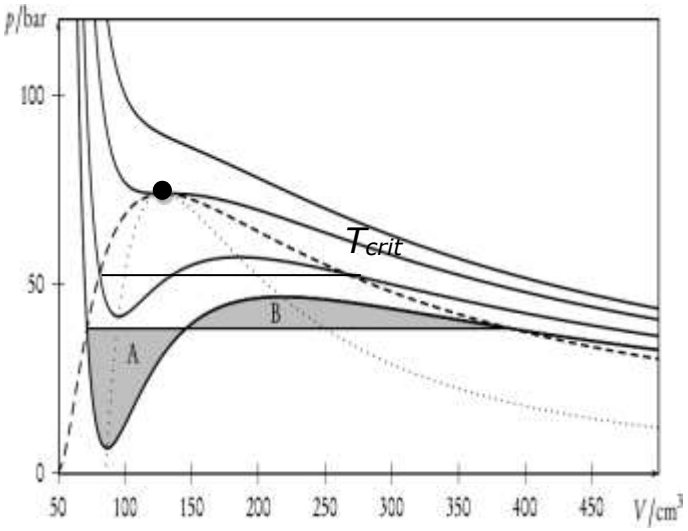

Figure 12: Van der Waals isotherms for CO_2 with spinodal (dotted) and binodal (dashed) curves. The dot marks the critical isotherm at critical pressure and volume. Hatched areas A and B=A illustrate the "Maxwell construction" to identify regions of phase coexistence in the p-V diagram.

Below the critical temperature, the pressure-density characteristics of a vdW gas at constant *T* implies a tendency for the gas to reduce resistance to external pressure. This effect leads to increased density and a more important attractive particle interactions.

Obviously, such a system is not stable. The gas "wants to" condense on its own, in the *P*-*V* region outlined by the "spinodal" curve in Figs. 10 and 12. As the volume of a gas sample at *T* is reduced, for example, by means of a constant external force (pressure p_{ext}) acting on a movable piston, it will partially undergo a transition to a denser phase, i.e., it will condense or ***liquefy***. For a given *T-const.*, a continuous isothermal process of liquefaction can start at a standard large volume, where the binodal intersects the isotherm. It ends at the smallest volume required to store the amount of matter in its liquified state. The latter volume defines the intersection of the binodal with the given isotherm. Of course, the process heat evolved will have to be taken up by a "heat bath" in thermal contact with the gas. Phase transitions will form subject of a later section.

For practical applications, the vdW EOS and similar models have been fitted to sets of sensitive experimental data for real gases, such as measured critical temperature and pressures, or points on binodal and spinodal curves. Calculations using the vdW EOS may

provide reasonable estimates of the behavior of real gases to be expected under given experimental conditions. Now the characteristic vdW or similar model parameters are known for many real gases. Because of the similarity of the underlying theoretical equation of state, all real gases behave essentially the same, if characterized by the macroscopic quantities p, V, T scaled with the respective critical values, e.g., T/T_{crit}, etc. (***Law of Corresponding States***)